Motional Time-Harmonic Simulation of Slotted Single-Phase Induction Machines

Herbert De Gersem, Karel De Brabandere, Ronnie J. M. Belmans, *Senior Member, IEEE*, and Kay Hameyer, *Senior Member, IEEE*

***Abstract*—Considering motional effects in the steady-state finite-element simulation of single-phase induction machines inevitably requires a transient approach. The resulting computation time seriously hampers the application of finite elements within technical designs. In this paper, time-harmonic finite-element simulation, as commonly applied to the three-phase induction machine model, is also enabled for single-phase motors by decomposing the air-gap field in two revolving fields in the opposite direction. The advantages and drawbacks of the novel approach are illustrated by a benchmark model. Issues such as ferromagnetic saturation, external circuit coupling, adaptive mesh refinement, and torque computation are addressed. The method is used to simulate a capacitor start/run motor.**

***Index Terms*—Ferromagnetic saturation, finite-element method, single-phase induction machine, time-harmonic simulation.**

I. Introduction

SINGLE-PHASE induction motors (IMs) are mainly used in domestic applications (e.g., in fans and lawn mowers [1]). They are preferred over their three-phase equivalents at places where only a single-phase ac supply is available as in most households [2]. Three-phase machines in Steinmetz connection can be operated at a single-phase grid as well [2]. Single-phase machine designs are very robust (either brushes or electronics) and can be mass-produced at relatively low cost. They, however, lack a self-starting capability and have a poor efficiency and power factor. Due to the present day concern to develop specialized cost-effective motors, improved designs of single-phase IMs are required. To that end, finite-element (FE) methods are expected to provide more accurate simulations compared to analytical and semianalytical approaches, especially if ferromagnetic saturation and eddy current effects are involved.

II. Existing Simulation Techniques for Single-Phase Induction Machines

A. Analytical Approaches

The wave spectra of the air-gap fields typical for three-phase IMs and single-phase IMs with and without auxiliary windings are plotted in Fig. 1. An analytical approach for three-phase IMs can consider equivalent circuits for stator and rotor parts. Then, only the fundamental air-gap field (i.e., the component with wave number $\lambda = 1$ is considered). The electrical phenomena in the rotor occur at the slip frequency

$$s_\lambda = \frac{\omega - \lambda\omega_m}{\omega} \tag{1}$$

with $\omega = 2\pi f$ the pulsation, f the frequency, and ω_m the mechanical speed, evaluated for $\lambda = 1$. The slip is the relative difference between the synchronous speed ω/λ of the rotating air-gap field and the mechanical velocity of the rotor. The magnetic coupling is introduced by applying an appropriate transformation dealing with the differences in number of turns and frequencies. The armature reaction is modeled by a slip-dependent resistance in the coupled electric circuit.

For single-phase devices, the reduction to a single harmonic is not acceptable. The components with the wave numbers $\lambda = 1$ (forward) and $\lambda = -1$ (backward) have to be at least considered. The analytical treatment of single-phase IMs relies on the decomposition of the alternating field into two synchronously revolving fields with half of the alternating field's magnitude and opposite direction [1]–[4]. The torque follows from the superposition of the speed-torque characteristics of two inversely excited, fictitious three-phase machines. An equivalent circuit is constructed from two three-phase machines, one at slip s_1 and one at slip s_{-1} [5]. This technique constitutes a comprehensive framework for qualitative evaluation of single-phase IMs. It is, however, not yet sufficient for obtaining reliable quantitative results. Many empirical correction factors have to be introduced [1]. Indeed, analytical approaches have difficulties to consider ferromagnetic saturation, eddy current effects, and arbitrary geometries. To this end, FE approaches are expected to be more accurate. The analytical approach, though, indicates the way toward a solution (i.e., by splitting the air-gap field into two reversely rotating components) and by introducing the slip transformation paradigm into the FE framework. The key point in the novel FE tool developed in this paper is the embedding of the decomposition of the air-gap field within the FE model.

B. Parameter Extraction

It is possible to rely on static and/or time-harmonic simulations to extract lumped parameters for an equivalent circuit model or a coupled inductor model of the single-phase machine. However, it remains cumbersome to incorporate ferromagnetic saturation and motional effects in the lumped parameter models.

Manuscript received August 30, 2001. This work was supported by the Belgian "Fonds voor Wetenschappelijk Onderzoek Vlaanderen" (G.0427.98), the Belgian Ministry of Scientific Research (IUAP P4/20), and the Research Council of the Katholieke Universiteit Leuven.

The authors are with the ESAT Department, ELEN Division, Katholieke Universiteit Leuven, Leuven, Belgium (e-mail: Herbert.DeGersem@esat.kuleuven.ac.be).

Publisher Item Identifier 10.1109/TEC.2002.802774.

C. Eulerian Formulation With Homogenization

For solid-rotor, single-phase IMs, the Eulerian formulation (i.e., explicitly modeling motional eddy currents by adding a convection term to the partial differential equation), provides the steady-state solution in a single computational step [6]. For slotted rotors, transient simulation can be avoided by the homogenization procedure proposed in [7]. However, homogenization leads to rather disappointing results for three-phase IMs. Similar nonreliable results should be expected for slotted single-phase machines. Hence, the Eulerian formulation is only recommended for solid-rotor single-phase IMs.

D. Transient FE Simulation

To account for all technically relevant phenomena in slotted single-phase IMs, a transient FE approach is up to the present inevitable, even for simulating steady-state operation. Transient FE approaches accounting for the external circuit and the mechanical motion of the single-phase IM are presented in [8] and [9]. The methods yield accurate results for all kinds of operating conditions. The required simulation times, however, are of the order of several hours up to a few days. As a consequence, this approach only serves advanced studies, but is of little use for common design and large-scale optimization. FE simulation is, however, expected to be a significant surplus for single-phase IM design. Its ability to consider the complicated geometries and winding schemes typical for electric machines is beneficial. The FE solution also indicates local ferromagnetic saturation, high current densities and, hence, local hot spots. The FE procedure can be fully automated and embedded within a parameter loop, a sensitivity analysis or an optimization routine [10]. This motivates the development of a relatively inexpensive but technically reliable FE method for the steady-state simulation of single-phase IMs, incorporating external circuits, all eddy current effects, and ferromagnetic saturation.

III. Time-Harmonic Simulation of Three-Phase Induction Machines

A common tool for three-phase IM analysis is a two–dimensional (2-D) FE method based on the time-harmonic magnetodynamic PDE

$$-\frac{\partial}{\partial x}\left(\nu\frac{\partial \underline{u}}{\partial x}\right)-\frac{\partial}{\partial y}\left(\nu\frac{\partial \underline{u}}{\partial y}\right)+\jmath\omega\sigma\underline{u}=\frac{\sigma}{\ell_z}\Delta\underline{V} \quad (2)$$

with $\mathbf{A}=(0,0,u)$ the magnetic vector potential, ν the reluctivity, σ the conductivity, ΔV the voltage drop applied between the front and rear ends of the device, and ℓ_z the length of the device. Underlined quantities indicate effective phasors. For example

$$u(t)=\mathrm{Re}\left\{\underline{u}\sqrt{2}e^{\jmath\omega t}\right\}. \quad (3)$$

The motional effects occurring in the rotor of a three-phase IM are considered by a simple trick similar as in equivalent circuit models. Currents at frequency f, applied to a two-pole stator winding, excite a magnetic flux with pulsation $\omega = 2\pi f$, rotating at the synchronous speed ω along the air gap of the device. An observer attached to the moving rotor, experiences all phenomena induced by this field in the rotor, at *slip frequency* $f_{s,1}=s_1 f$ [11]. Hence, for the fundamental field, the induced effects in a moving rotor are a factor s_λ smaller when compared to the effects observed at standstill. As a consequence, the motional simulation is equivalent to the standstill simulation of a rotor with rotor bars featuring the fictitious conductivities $s_\lambda\sigma$ instead of the true conductivities σ in (2) [12]. The *slip transformation* enables the steady-state time-harmonic simulation of a three-phase IM with slotted stator and rotor by simply adjusting the conductivities. Hence, for steady-state simulation, expensive transient simulation is avoided. Although the time-harmonic approach with slip transformation neglects the induced currents due to the spatial harmonic distribution in the air gap, it achieves a sufficient accuracy for the design of many practical three-phase IMs [13].

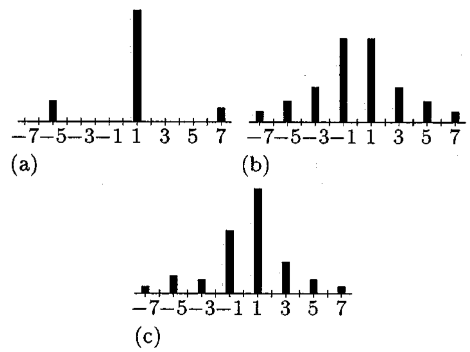

Fig. 1. Typical wave spectra of (a) a rotating field in a three-phase IM, (b) an alternating field in a single-phase IM, and (c) an elliptical field in a capacitor motor.

For three-phase IMs, the slip transformation technique is validated by the dominance of the fundamental air-gap field (Fig. 1). In case of a single-phase IM, the air gap contains a significant field rotating in the opposite direction as well. Hence, besides the phenomena at slip frequency, also a component at the frequency $f_{s,-1}=s_{-1}f$ is induced in the rotor and is responsible for a nonnegligible torque generation [2]. As a consequence, the slip transformation approach known from three-phase IM analysis does not directly carry over the time-harmonic FE simulation of single-phase IMs. Therefore, for the simulation of steady-state operation, a transient FE approach is inevitable [8], [9].

IV. Air-Gap Flux Splitting

The principle of air-gap flux splitting within a FE model is presented here in a technical way. A more mathematical formulation is offered in [14]. The purpose of air-gap flux splitting is the decomposition of the air-gap field in order to enable the application of slip transformation with respect to forward and backward rotating components independently. In addition, the continuity of the normal component of the magnetic flux density and the continuity of the tangential component of the magnetic field strength have to be preserved.

The FE model consists of one stator and two rotor models, denoted by $\Omega_{\&}$, Ω_{+}, and Ω_{-}. The boundaries $\Gamma_{\&}$, Γ_{+}, and Γ_{-} match at an interface in the air gap (Fig. 2). For convenience, an equidistant and matching grid with $2m$ grid points is constructed

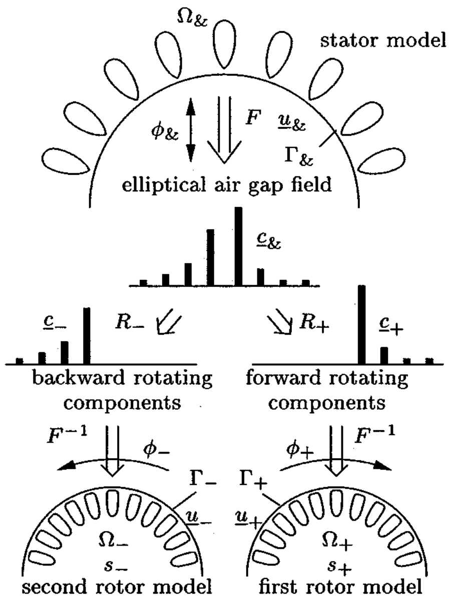

Fig. 2. Scheme of the air-gap flux splitting approach.

along $\Gamma_\&$, Γ_+, and Γ_-. The magnetic vector potential $\underline{u}_\&$ along $\Gamma_\&$ is transformed in its Fourier coefficients $\underline{c}_\&$: $\underline{c}_\& = F\underline{u}_\&$ with $\underline{c}_\& = \{\underline{c}_\lambda, \lambda = -m+1, \ldots, m\}$ and F the Fourier transform operator. The coefficient vector $\underline{c}_\&$ is split into two coefficient vectors $\underline{c}_+$ and $\underline{c}_-$ containing for the forward ($\lambda > 0$) and backward ($\lambda \leq 0$) rotating components, respectively. The corresponding restriction operators are denoted by R_+ and R_-, i.e., $\underline{c}_+ = R_+\underline{c}_\&$ and $\underline{c}_- = R_-\underline{c}_\&$. The forward rotating components are propagated to the rotor model Ω_+ (right in Fig. 2), whereas the backward rotating components are applied to the rotor model Ω_- (left in Fig. 2). At Γ_+ and Γ_-, the decomposed fields $\underline{u}_+$ and $\underline{u}_-$ are restored by inverse Fourier transforms (i.e., $\underline{u}_+ = F^{-1}\underline{c}_+$ and $\underline{u}_- = F^{-1}\underline{c}_-$). Equidistant and matching grids at the air-gap interface are recommended as the possibility of applying the fast Fourier transform (FFT) algorithm substantially reduces the computational cost of the method.

The relations between $\underline{u}_\&$, $\underline{u}_+$, and $\underline{u}_-$ are summarized in the constraint equation

$$\underbrace{\begin{bmatrix} 0 & R_+F & -F & 0 \\ 0 & R_-F & 0 & -F \end{bmatrix}}_{B} \underbrace{\begin{bmatrix} \underline{u}_o \\ \underline{u}_\& \\ \underline{u}_+ \\ \underline{u}_- \end{bmatrix}}_{\underline{u}} = \begin{bmatrix} 0 \\ 0 \end{bmatrix} \tag{4}$$

with $\underline{u}_o$ the FE degrees of freedom strictly in $\Omega_\& \cup \Omega_+ \cup \Omega_-$. The introduction of the additional constraints in the FE system of equations gives rise to the saddle-point problem

$$\begin{bmatrix} K & B^* \\ B & 0 \end{bmatrix} \begin{bmatrix} \underline{u} \\ \underline{p} \end{bmatrix} = \begin{bmatrix} \underline{f} \\ 0 \end{bmatrix} \tag{5}$$

with K and $\underline{f}$ the FE stiffness matrix and load vector obtained by discretising (2) and $\underline{p}$ a set of Lagrange multipliers [14]. The procedure sketched before ensures the continuity of $\underline{u}$ (i.e., $\underline{u}_\& = \underline{u}_+ + \underline{u}_-$) which is equivalent to the continuity of the normal component of the magnetic flux density. The continuity of the tangential component of the magnetic field strength is implicitly fulfilled by (5).

Once decomposed, observers attached to both rotor models each experience one dominant component: the observer attached to Ω_+ experiences the dominant forward rotating component $F^{-1}\underline{c}_1$ at Γ_+ whereas the observer attached to Ω_- experiences the dominant backward rotating component $F^{-1}\underline{c}_{-1}$ at Γ_-. Two slip values are determined with respect to each of these components independently: $s_+ = s_1$ and $s_- = s_{-1}$. Note that $s_+ = 2 - s_-$. Moreover, $s_+ = s_-$ only if $\omega_m = 0$. Hence, the FE stiffness matrix parts associated with Ω_+ and Ω_-, in general, are different. Motional eddy current effects with respect to the fundamental forward and backward rotating waves are correctly taken into account. The true solution in the rotor is approximated by the sum of the solutions in both rotor models.

The air-gap flux splitting method with slip transformation is applicable to all kind of devices, featuring an alternating or an elliptical air-gap field, such as run, run/start, start capacitor motors, shaded-pole IMs, and three-phase IMs with unbalanced excitations. There is no need to estimate the ellipticity of the air-gap field in advance. The method automatically computes the magnitudes and phases of both rotating components by solving (5).

Since the slip is only determined according to the fundamental rotating components, the induced phenomena due to the higher harmonic contents are not correctly taken into account. Here, the same uniformity condition applies to the air-gap field as in the case of a three-phase IM. The fact that the higher harmonic content of a single-phase IM air-gap field is considerably higher then the one of a three-phase machine, indicates the main approximation introduced by the air-gap flux splitting and slip transformation method described.

V. Benchmark Model

The procedure is illustrated by a benchmark single-phase IM model consisting of a stator yoke with one winding and a solid rotor [15]. The particular geometry and excitation enables an analytical solution used for comparison [16]. The excitation current layer contains, besides the fundamental alternating field, a considerable amount of significant higher harmonics. The FE model is presented in Fig. 3. The forward and backward air-gap waves are distributed to two different rotor models. Motional eddy current effects are accounted for by slip transformation. The slip s_1 of the mechanical rotation with respect to the fundamental forward component is multiplied to the rotor conductivity. As in the other rotor model, in general, a different factor s_{-1} is used, the reaction of both rotor models to the air-gap field differs. In a post-processing step, both fields are superposed and represented upon the additional rotor mesh centered within the stator. This is a representation of the true field in the rotor of the single-phase IM. It is interesting to have a look at the field at time t_0 and at time $t_1 = t_0 + T/4$, a quarter of a period $T = 1/f$ later. Both partial solutions establish at t_1 a solution approximately resembling the one at t_0 rotated over 90° mechanically, which indicates their rotation. The superposed solution is, however, mainly alternating, with its maximum approximately at t_0 and almost vanishing at t_1.

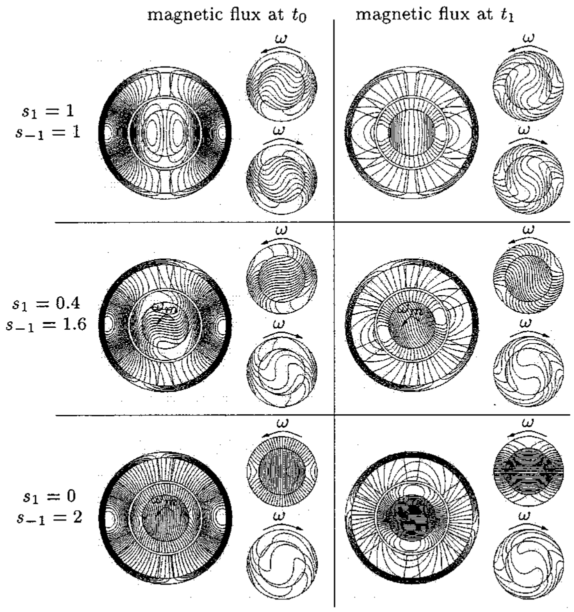

Fig. 3. Benchmark single-phase IM: magnetic flux plot for a slip of (a) 1, (b) 0.4, and (c) 0 at t_0 (left) and t_1 (right).

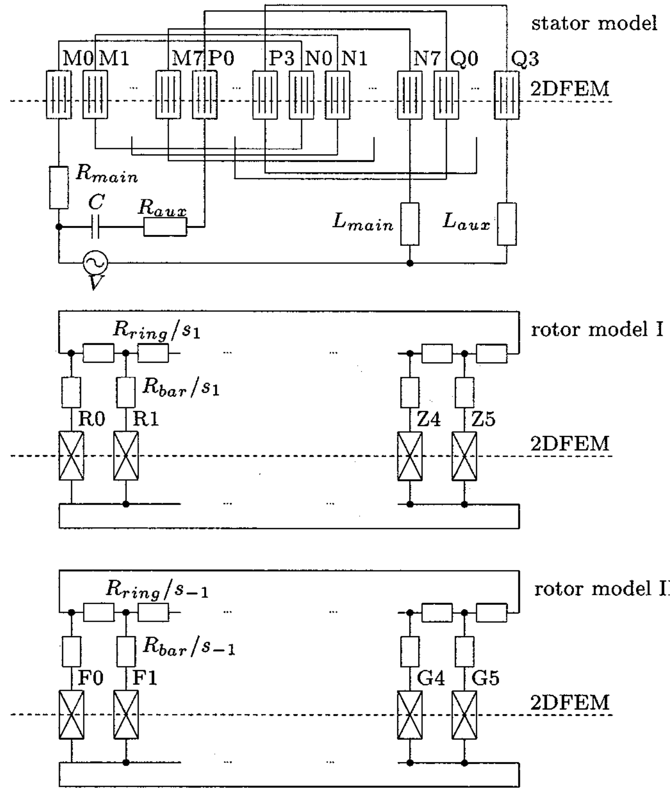

Fig. 4. External circuit connections of the start/run-capacitor single-phase IM.

At standstill, both rotors feature the same conductivity and, hence, react the same way to the applied rotating fields [Fig. 3(a)]. In Fig. 3(c), the motor operates at theoretical no-load. Hence, the forward air-gap field is synchronous with respect to the mechanical velocity and no currents are induced. The other rotor has a slip $s_{-1} = 2$ and adds a small reaction field, causing a small braking torque. The simulation can be repeated for all steady-state operations of the single-phase IM [Fig. 3(b)]. Each time, the flux is divided to both rotor models and the magnetomotive force (MMF) depends upon their reaction fields determined by the values for the slip. The assumption of a pure sinusoidal air-gap field is not entirely true. This is reflected by the slight differences between the rotating parts at t_0 and t_1. Due to the concentrated stator winding, this benchmark model has a relatively large harmonic distortion in the air gap when compared to technical devices. It is, however, expected that this approach is sufficiently accurate for technical models.

VI. Ferromagnetic Saturation

The approach presented here is based on the superposition principle, implicitly assuming linear material characteristics. It is known that ferromagnetic saturation of the stator and rotor iron has a significant influence on the system's performance. Hence, it is important to consider this phenomenon in the simulation of technical single-phase IMs. A successive substitution strategy is used to incorporate nonlinear materials in the approach with air-gap flux splitting. A similar method has been developed in [13] to deal with nonlinear material characteristics when using black-box FE software. First, a linear solution is obtained. The true field is constructed on the mesh of the middle rotor by the superposition of both partial solutions of the other rotors. To the superposed field, the effective saturation characteristic is applied [17]. Afterwards, the obtained reluctivities are projected on the left and right rotor models before performing the next step in the nonlinear iteration. To prevent divergence or oscillations of the nonlinear process, under-relaxation is applied to the reluctivities between two successive steps.

VII. Adaptive Mesh Refinement

An automatic control of the discretization error is provided by adaptive mesh refinement. An error estimator indicates FEs for which a large error is expected. The mesh refiner subdivides the marked elements and restores the conformity and the mesh quality. This process is applied for both rotors independently. The error indication depends on the local importance of eddy current effects. Though originally the same, the meshes of the two rotor models may become considerably different due to mesh adaptation. The middle rotor does not participate in the solution process itself. Nevertheless, it is necessary to refine the middle rotor model accordingly in order to ensure the consistency of the FE discretization. In order to achieve optimal use of degrees of freedom, one preferably refines elements of the middle rotor with large flux densities and, thus, with significant saturation. Since the rotor meshes are nonmatching, mesh projection techniques have to be applied while restoring the true field on the middle rotor and returning the material data to the left and right rotors.

VIII. Torque Computation

The improved Maxwell stress tensor method presented in [18], is an efficient method to compute the torque of rotating devices. The improved Maxwell stress tensor method is invoked in the three partial air-gap regions attached to each of the rotor

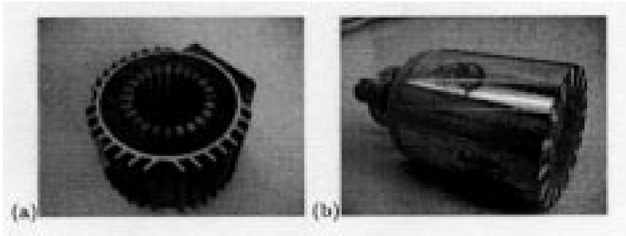

Fig. 5. (a) Stator and (b) rotor of the capacitor motor.

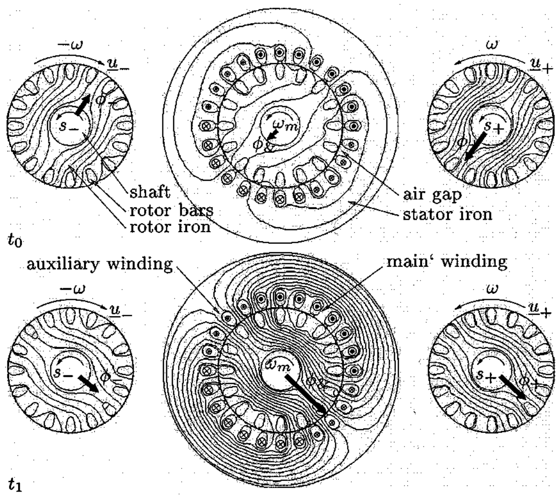

Fig. 6. Plot of the magnetic flux lines at t_0 and t_1 of the start/run-capacitor motor model operating at slip 0.5.

and stator models. The three values of the torque correspond to the torques of the fictitious three-phase IMs and their sum, constituting the true torque generated by the single-phase IM.

IX. External Electric Circuit

As for three-phase devices, it is important to account for the additional impedances of the rotor end rings and the stator end windings which are not incorporated in the 2-D FE model [13]. The auxiliary winding of split-phase IMs is connected to a capacitor (seldom to a resistor or inductor). The single-phase IM is embedded into a supply circuit. The 3-D effects due to end windings and end rings, are modeled by lumped parameters. The electrical connections are resolved by a circuit model which adds additional algebraic equations to the FE system matrix [19]. For a capacitor motor, the stator part consists of a main and auxiliary winding, represented by stranded conductors (Fig. 4). The splitting approach amounts to considering two distinct circuits connecting the rotor bars: one for all phenomena at frequency $s_1 f$ and one for all phenomena at frequency $s_{-1} f$.

X. Application: Capacitor Start/Run Motor

The flux splitting approach presented here is applied to simulate a start/run capacitor single-phase IM (Fig. 5). In a capacitor motor, the alternating field excited by the main winding is augmented by an air-gap field generated by an auxiliary winding, geometrically placed in the axis in quadrature to the main winding and excited by the same single-phase supply through a capacitor (Fig. 4). Both windings are single-layer windings. The main winding occupies 16 stator slots whereas the auxiliary winding fills the remaining eight slots (Fig. 6). The rotor comprises 16 aluminum rotor bars. The model is constructed similarly to the benchmark model. The middle rotor serves the purpose of superposing the solutions of the other rotor models, evaluating the nonlinear characteristic of the ferromagnetic iron, and visualizing the final solution. The motion of the rotor is considered by multiplying the conductivity of the rotor bars by the slip s_1 for the right rotor and by s_{-1} for the left rotor. In Fig. 6, the magnetic flux line plots for the capacitor motor operating at $s_1 = 0.5$ are shown.

XI. Conclusions

The elliptical air-gap flux, typical for single-phase induction machines, is decomposed within an FE model in its forward and backward rotating components. The left rotating components are applied to a rotor model, considering the phenomena at slip frequency. A separate rotor model deals with the high frequent currents induced by the inverse rotating component. The superposition of both fields constitutes the true rotor field. The model is equipped with a nonlinear loop that accounts for ferromagnetic saturation, adaptive mesh refinement, a torque computation routine, and external circuit coupling. The novel time-harmonic FE approach for single-phase IM simulation avoids expensive transient computation for steady-state simulation. The application to a capacitor motor reveals that this approach offers sufficient technical accuracy.

References

[1] C. G. Veinott, *Fractional- and Subfractional-Horsepower Electric Motors*, 3rd ed. New York: McGraw-Hill , 1970.
[2] H.-D. Stölting and A. Beisse, *Elektrische Kleinmaschinen*. Stuttgart: B. G. Teubner, 1987.
[3] J. Štěpina, *Die Einphasen-asynchronmotoren*. Wien, Austria: Springer-Verlag, 1982.
[4] S. Williamson and A. C. Smith, "A unified approach to the analysis of single-phase induction motors," *IEEE Trans. Ind. Applicat.*, vol. 35, pp. 837–843, July 1999.
[5] A. M. Stankovic, B. C. Lesieutre, and T. Aydin, "Modeling and analysis of single-phase induction machines with dynamic phasors," *IEEE Trans. Power Syst.*, vol. 14, pp. 9–14, Feb. 1999.
[6] H. De Gersem and K. Hameyer, "Comparison of motional and nonmotional time-harmonic finite element simulations of solid rotor single-phase induction machines," in *Proc. IEEE Conf. Electromagn. Field Comput.* , Milwaukee, WI, June 2000, p. 108.
[7] ——, "Finite element simulation of motional eddy currents in slotted geometries," 10th Intl. Sym. Applied Electro. Mech. , pp. 97–98, May 13–16, 2001, submitted for publication.
[8] C. B. Rajanathan and B. J. Watson, "Simulation of a single phase induction motor operating in the motoring, generating and braking modes," *IEEE Trans. Magn.*, vol. 32, pp. 1541–1544, May 1996.
[9] N. Sadowski, R. Carlson, S. R. Arruda, C. A. da Silva, and M. Lajoie-Mazenc, "Simulation of single-phase induction motor by a general method coupling field and circuit equations," *IEEE Trans Magn.*, vol. 31, pp. 1908–1911, May 1995.
[10] U. Pahner, R. Mertens, H. De Gersem, R. Belmans, and K. Hameyer, "A parametric finite element environment tuned for numerical optimization," *IEEE Trans. Magn.*, vol. 35, pp. 2936–2939, Sept. 1998.
[11] W. Nürnberg, *Die Asynchronmaschine*, 2nd ed. Wien, Austria: Springer-Verlag, 1963.
[12] E. Vassent, G. Meunier, and J. C. Sabonnadière, "Simulation of induction machine operation using complex magnetodynamic finite elements," *IEEE Trans. Magn.*, vol. 25, pp. 3064–3066, July 1989.

[13] R. De Weerdt, E. Tuinman, K. Hameyer, and R. Belmans, "Finite element analysis of steady state behavior of squirrel cage induction motors compared with measurements," *IEEE Trans. Magn.*, vol. 33, pp. 2093–2096, Mar. 1997.

[14] H. De Gersem and K. Hameyer, "Air-gap flux splitting for the time-harmonic finite-element simulation of single-phase induction machines," *IEEE Trans. Magn.*, vol. 38, pp. 1221–1224, Mar. 2002.

[15] K. Davey, "Rotating field analysis using boundary element method," *IEEE Trans. Magn.*, vol. 35, pp. 1402–1405, May 1999.

[16] ——, "Analytic analysis of single- and three-phase induction motors," *IEEE Trans. Magn.*, vol. 34, pp. 3721–3727, Sept. 1998.

[17] D. Lederer, H. Igarashi, and A. Kost, "Modeling of nonlinear magnetic material using an effective permeability—comparison between different formulations," *ACES J.*, vol. 12, pp. 113–116, July 1997.

[18] K. Hameyer, R. Mertens, U. Pahner, and R. Belmans, "New technique to enhance the accuracy of 2-d/3-d field quantities and forces obtained by standard finite-element solutions," *Proc. Inst. Elect. Eng. Sci. Measu. Technol.*, vol. 145, no. 2, pp. 67–75, Mar. 1998.

[19] H. De Gersem, R. Mertens, U. Pahner, R. Belmans, and K. Hameyer, "A topological method used for field-circuit coupling," *IEEE Trans. Magn.*, vol. 34, pp. 3190–3193, Sept. 1998.

Herbert De Gersem received the M.Sc. and Ph.D. degrees in electrical engineering from the Katholieke Universiteit Leuven, Leuven, Belgium, in 1994 and 2001, respectively.

From 1995 to 2001, he worked as a research assistant with the research group Electrical Energy at the same university. Since March 2001, he has been with the Computational Electromagnetics Laboratory, University of Technology, Darmstadt, Germany. His research interests are electromagnetic field simulation using hybrid finite-element methods and domain decomposition and multigrid techniques applied to electrical energy transducers, in particular, electrical machines and superconductive magnets.

Karel De Brabandere received the M.Sc. degree in electrotechnical engineering from the Katholieke Universiteit Leuven, Leuven, Belgium, where he is currently working as a research assistant and pursuing the Ph.D. degree on the subject of control algorithms for active filters and switched reluctance drives.

His interests include power electronics, drives, and power quality.

Ronnie J. M. Belmans (SM'89) received the M.Sc. and Ph.D. degrees in electrical engineering in 1979 and in 1984, respectively, from the Katholieke Universiteit Leuven (K.U. Leuven) Energy Institute, Leuven, Belgium, and the Special Doctorate degree in 1989 and the Habilitierung, in 1993, both from the RWTH, Aachen, Germany.

From 1979 to 1985, he was a member of the staff of the K.U. Leuven Energy Institute. Currently, he is a Full Professor with K.U. Leuven, teaching electrical machines, variable-speed drives, and computer-aided design (CAD) in magnetics. His research interests include electrical machine design, computer-aided engineering, variable-speed drives, as well as vibrations and audible noise in electrical machines. He is also performing research on the system aspect of the liberalization of the electricity market. He was with the Laboratory for Electrical Machines of the RWTH as a Von Humboldt Fellow from October 1988 to September 1989. From October 1989 to September 1990, he was a Visiting Associate Professor at McMaster University, Hamilton, ON, Canada. From 1995 to 1996, he occupied the Chair at London University, London, U.K., offered by the Anglo-Belgian Council. Since 1997, he has been a visiting Professor at RWTH and, since 1999, at Imperial College, London. In addition, since 1997, he has been President of the International organization on Electricity Use (UIE), Paris, France. He is director of several basic and industrial research projects. Currently, he is head of the Electrical Engineering Department and is the vice president of the K.U. Leuven Energy Institute.

Dr. Belmans is a Fellow of the IEE (U.K.) and a member of the Koninklijke Vlaamse Ingenieursvereniging (kVIV).

Kay Hameyer (SM'99) received the M.Sc. degree in electrical engineering from the University of Hannover, Hannover, Germany. He received the Ph.D. degree from University of Technology (TU Berlin), Berlin, Germany.

After his university studies, he worked with the Robert Bosch GmbH, Stuttgart, Germany, as a design engineer for permanent magnet servo motors. In 1988, he became a member of the staff at TU Berlin. In 1992, he was a visiting Professor at the COPPE Universidade Federal do Rio de Janeiro, Rio de Janeiro, Brazil, teaching electrical machine design and numerical techniques. In the frame of collaboration with TU Berlin, he was, in 1993, a Visiting Professor at the Université de Batna, Batna, Algeria. Beginning in 1993, he was a scientific consultant working on several industrial projects. From 1993 to March 1994, he held a HCM-CEAM fellowship financed by the European Community and worked at the Katholieke Universiteit Leuven (K.U. Leuven) Energy Institute, Leuven, Belgium. From 1996 to 2000, he was a Senior Researcher with the F.W.O.V. in Belgium. Since 1996, he has been a Professor of numerical field computations and electrical machines and drives with the K.U. Leuven Energy Institute, teaching numerical techniques in electrical engineering, drive technology, and electrical machines. His research interests are numerical field computation and the design of electrical machines, in particular, permanent magnet excited machines, induction machines, and numerical optimization strategies.

Dr. Hameyer is a member of the International Compumag Society, a member of the Belgian Royal Society of Engineers K-VIV, and a member of the IEE.